Photochemical Incorporation of Silver Quantum Dots in Monodisperse Silica Colloids for Photonic Crystal Applications

Wei Wang and Sanford A. Asher*

Contribution from the Department of Chemistry, University of Pittsburgh, Pittsburgh, Pennsylvania 15260

Received May 22, 2001

Abstract: We developed a novel method to fabricate nanocomposite monodisperse SiO_2 spheres (∼100 nm) containing homogeneously dispersed Ag quantum dots (2∼5 nm). The inclusion morphology is controlled through the timing of the photochemical reduction of silver ions during hydrolysis of tetraethoxysilane in a microemulsion. Depending on the timing, Ag quantum dots can be directed to different annuli within the SiO_2 spheres, as well as onto the SiO_2 sphere surfaces. The embedded Ag quantum dots show a plasmon resonance absorption band at 438 nm. These Ag@SiO_2 particles have significant surface charge and readily self-assemble into crystalline colloidal array (CCA) photonic crystals which Bragg-diffract light in the visible region. The magnitude of the plasmon resonance absorption depends on the CCA Bragg diffraction condition. The negative dielectric constant of the silver nanoparticles may be decreasing the silica−silver nanodot composite refractive index below that of the water medium. We may be observing an analogue of the Borrmann effect previously observed in X-ray scattering, where the incident and diffracted electric field standing wave becomes localized in regions of small CCA crystal absorption.

Nanoscale metal and semiconductor particles are of current interest because they mark a material transition range between quantum and bulk properties.[1] With decreasing particle size, bulk properties are lost as the continuum of electronic states becomes discrete (i.e. quantum size effect) and as the fraction of surface atoms becomes large.[2] The electronic and magnetic properties of metallic nanoparticles and nanoclusters show new properties,[3] which can be utilized in novel applications in areas that range from nonlinear optical switching, and catalysis, to high-density information storage, for example.[4]

Numerous methods have been developed to synthesize metal nanoparticles.[4] A major difficulty with scale-up of these methods is that the metal colloid stability is often controlled by electrostatic interactions across the Debye double-layer, and sterically through the adsorption of steric stabilizing agents such as polymers and surfactants. Thus, the metal colloids are very sensitive to their environment.

One way to improve the stability of the metal nanoparticles is to coat them with silica, which is very resistant to coagulation, even at high-volume fractions. Recently, Mulvaney et al.[5] and Matijević et al.[6] reported that noble metal particles such as Ag and Au could be coated with silica shells. However, these silica-coating procedures usually involved a multistep process, and only single metal particle cores could be coated.[5,6]

We previously developed a flexible microemulsion synthetic method to prepare silica−CdS composites that could be tailored to yield a variety of morphologies.[7] More recently, Li et al.[8] used a similar approach to prepare SiO_2 spheres with a single Ag core. However, their microemulsion recipe limited the resulting SiO_2 sphere to a maximum diameter of ∼55 nm. In addition, these silver−silica core−shell composite particles had relatively large silver core sizes (10−60 nm) where the silver begins to show more bulk property behavior. These synthetic methods were also unable to fabricate silica spheres with homogeneously dispersed metal quantum dots.

We attempted to include Ag or Au quantum dots in silica spheres by the in situ chemical reduction of these ions in a microemulsion during the hydrolysis of the tetraethoxysilane (TEOS) using methods which worked well for CdS.[7] However, the metal particles aggregated and precipitated, resulting in the incorporation of few metal particles into the silica spheres.

We report here a novel method to fabricate nanocomposite SiO_2 colloidal particles containing homogeneously dispersed Ag quantum dots. The morphologies of the inclusions are controlled through the photochemical reduction of silver ions, instead of chemical reduction, in a microemulsion reaction matrix during

* To whom correspondence should be addressed. E-mail: asher@pitt.edu.

(1) (a) Alivisatos, A. P. *J. Phys. Chem.* **1996**, *100*, 13226. (b) Henglein, A. *Ber. Bunsen-Ges. Phys. Chem.* **1997**, *101*, 1562. (c) Markovich, G.; Collier, C. P.; Henrichs, S. E.; Remacle, F.; Levine, R. D.; Health, J. R. *Acc. Chem. Res.* **1999**, *32*, 415.

(2) (a) Rosetti, R.; Hull, R.; Gibson, J. M.; Brus, L. E. *J. Chem. Phys.* **1985**, *82*, 552. (b) Ricard, D.; Roussignol, P.; Flytzanis, C. *Opt. Lett.* **1985**, *10*, 511.

(3) (a) Lopez-Quintela, M. A.; Rivas, J. *Curr. Opin. Colloid Interface Sci.* **1996**, *1*, 806. (b) Mulvaney, P. In *Semiconductor Nanoclusters*; Kamat, P. V., Meisel, D. Eds.; Studies in Surface Science and Catalysis, Vol. 103; Elsevier Science B.V.: The Netherlands, 1996; p 99. (c) Rao, C. N. R.; Kulkarni, G. U.; Thomas, P. J.; Edwards, P. P. *Chem. Soc. Rev.* **2000**, *29*, 27.

(4) Belloni, J. *Curr. Opin. Colloid Interface Sci.* **1996**, *1*, 184.

(5) (a) Liz-Marzán, L. M.; Giersig, M.; Mulvaney, P. *Langmuir* **1996**, *12*, 4329. (b) Giersig, M.; Liz-Marzán, L. M.; Ung, T.; Su, D.; Mulvaney, P. *Ber. Bunsen-Ges. Phys. Chem.* **1997**, *101*, 1617.

(6) Hardikar, V. V.; Matijević, E. *J. Colloid Interface Sci.* **2000**, *221*, 133.

(7) (a) Chang, S.; Liu, L.; Asher, S. A. *J. Am. Chem. Soc.* **1994**, *116*, 6739. (b) Chang, S.; Liu, L.; Asher, S. A. *J. Am. Chem. Soc.* **1994**, *116*, 6745.

(8) Li, T.; Moon, J.; Morrone, A. A.; Mecholsky, J. J.; Talham, D. R.; Adair, J. H. *Langmuir* **1999**, *15*, 4328.

10.1021/ja011262j CCC: $20.00
Published on Web 11/22/2001

the hydrolysis of TEOS. Depending on the timing of the photochemistry the Ag quantum dots can be directed to different annuli within the SiO_2 spheres as well as onto the SiO_2 sphere surface or both. These particles have significant surface charge and readily self-assemble into crystalline colloidal arrays (CCA) which Bragg-diffract light. We observe that the silver plasmon absorption detected by transmission measurements depends on the Bragg diffraction condition of these CCA photonic crystals.

Experimental Section

Materials. $AgNO_3$ (99+%), Igepal CO-720, and hexanol (98%) were purchased from Aldrich. Tetraethoxysilane (TEOS, ≥ 99%) was purchased from Fluka. Cyclohexane (GC, 99%) and isopropyl alcohol (GR) were from EM Sciences. Absolute methanol (AR) was obtained from Mallinckrodt. $NH_3 \cdot H_2O$ (29.5%) and dimethyl sulfoxide (99.9%) was obtained from J.T. Baker. DOWEX MR-3 mixed bed ion-exchange resin was obtained from Dow Chemical Co. All chemicals were used as received. The ~17.9 MΩ·cm resistivity water was obtained from a Barnstead Nano-pure water purifier.

Measurements. Optical transmission spectra were taken with a Lambda 9 UV−visible/near-IR spectrophotometer. Particle polydispersities and ζ potentials were determined by using a Brookhaven ZetaPALS ζ potential analyzer. A 1 mM KCl solution was used as the medium for the ζ potential measurements. The ζ potential calculation employed the Smoluchowski equation, which assumes the particle radii are much larger than the double layer thickness.[9]

A Zeiss 902 electron microscope were used to image the particles. A drop of the dilute particle suspension was placed on a Formvar/carbon film supported by a copper grid (Ted Pella, Inc.), and the solvent was allowed to evaporate. Sphere size distributions were obtained by digitizing the printed micrographs and analyzing 300 particles using the public domain NIH Image 1.60 software (http://rsb.info.nih.gov/nih-image/).

Synthesis. The colloidal particles were synthesized within a microemulsion prepared by using Igepal CO-720.[7] For a typical preparation we prepared the Ag^+ ion containing microemulsion by adding 10.7 mL of a freshly prepared 1.0 M $AgNO_3$ aqueous solution under rapid stirring to a solution prepared from 27.5 g of Igepal CO-720, 22.0 mL of hexanol, 170 mL of cyclohexane, and 3.0 mL of $NH_3 \cdot H_2O$ (29.5%). After the microemulsion became optically clear we injected 20 mL of TEOS. TEOS is the preferred silica precursor due to its relatively slow reaction rate. The reaction mixture was stirred for 24 h at ambient temperature.

Exposure of the reaction mixture to UV light from a Blak Ray mercury lamp (365 nm) results in an increasing yellow solution, due to the photochemical reduction of Ag^+. During this interval the TEOS slowly hydrolyzes. We presume that the $Si(OH)_4$ precipitates and condenses onto the metal particles within the microemulsion water nanopools to form the monodisperse Ag@SiO_2 composite spheres. The final morphology depends on the UV light illumination intensity, time, and the initial concentration of silver ions. In the absence of silver ions, the recipe produces pure white ~100 nm diameter SiO_2 spheres.

After the reactions were complete, the microemulsions were destabilized by adding 2-propanol. The lotion-like precipitate was separated by centrifugation. The resulting particles were further washed twice each with 2-propanol, cyclohexane, methanol, and pure water. These cleaning cycles utilized a vortex mixer and ultrasonication to redisperse the particles. Centrifugation was used after each wash to harvest the particles.

Results and Discussion

In the absence of UV light, freshly prepared Ag^+ ions are stable in the reaction microemulsion mixture. Completion of the hydrolysis and condensation of TEOS in the microemulsion mixture results in a white colloidal dispersion. As shown in Figure 1A the product is essentially pure SiO_2 spheres without visible Ag inclusions. Even under ambient room light, almost no Ag quantum dots form during a reaction using freshly prepared Ag^+ solution. The TEM of particles synthesized with Ag^+ but not illuminated with UV light appear similar to those synthesized in the absence of Ag^+.

Photochemical reduction has been used previously to prepare metal colloids.[10] UV irradiation of aqueous solutions of Ag^+ induces photooxidation of water by excited Ag^+, resulting in the formation of silver atoms Ag^0, H^+, and OH• radicals.[11] Subsequent agglomeration of Ag^0 produces silver clusters $(Ag^0)_n$ and colloidal silver $(Ag^0)^c$.

$$Ag^+ + H_2O \xrightarrow{h\nu} Ag^0 + H^+ + OH\bullet$$

$$nAg^0 \rightarrow (Ag^0)_n \rightarrow (Ag^0)^c$$

Exposing the fresh Ag^+-containing microemulsion medium to UV irradiation for the first 12 h of a 24 h TEOS hydrolysis reaction results in a yellow colloidal dispersion. The Figure 1B TEM photograph shows that 2−5 nm Ag nanoparticles are homogeneously incorporated into the ~95 nm SiO_2 spheres.

The morphology of the composite particles strongly depends on the time history of exposure to UV light. For example, if UV illumination occurs only late in the reaction, such as over the last 12 h, large Ag particles appear on the SiO_2 sphere surface. Surprisingly, Ag quantum dots are also found within the SiO_2 spheres, even though the sphere growth had almost ceased after 12 h (Figure 1C). This indicates that Ag^+ photoreduction is occurring deep within the silica particles and that Ag quantum dots can form deep within the silica spheres.

Figure 1C also suggests that fewer Ag quantum dots are incorporated if the illumination occurs during the last half of the reaction. Indeed, if the UV illumination is only applied very late in the reaction, during the last 4 h, Ag particles only deposit near the SiO_2 surface (Figure 1D). This suggests that the silica sphere morphology is changing in the latter half of the reaction; this morphology change prevents silver quantum dot growth with the spheres.

If the reaction microemulsion is exposed to UV light for the first 4 h of the reaction, and is then kept in the dark for the remaining 20 h, the Ag quantum dots are enriched close to the SiO_2 sphere center (Figure 1E). Few Ag particles occur in the outer shell, because Ag nanoparticles were not formed during the outer shell growth.

If we use an aged $AgNO_3$ solution (>5 days old) we immediately observe a slight yellowing of the reaction mixture, presumably due to formation of a small quantity of silver colloid. This may result from the surfactant-induced agglomeration of the small silver clusters which formed in the aged Ag^+ solution.

A reaction in the dark using an aged Ag^+ solution results in only a small amount of Ag quantum dots occurring within the SiO_2 spheres (Figure 1F). In contrast an aged Ag^+ solution can be photochemically reduced by visible light to form Ag quantum dots throughout the silica sphere (Figure 2A). Visible light is presumably absorbed by the existing Ag quantum dots, and the resulting photooxidization of water gives rise to further Ag^+ reduction.

(9) Hiemenz, P. C. *Principles of Colloid and Surface Chemistry*, 2nd ed.; Marcel Dekker: New York, 1986; Chapter 13.

(10) (a) Ershov, B. G.; Henglein, A. *J. Phys. Chem.* **1993**, *97*, 3434. (b) Henglein, A.; Mulvaney, P.; Holtzworth, A.; Sosebee, T.; Fojtik, A. *Ber. Bunsen-Ges. Phys. Chem.* **1992**, *96*, 754. (c) Barnickel, P.; Wokaun, A.; Sager, W.; Eicke, H. F. *J. Colloid Interface Sci.* **1992**, *148*, 80. (d) Barnickel, P.; Wokaun, A. *Mol. Phys.* **1990**, *69*, 1. (e) Yonezawa, Y.; Sato, T.; Kuroda, S.; Kuge, K. *J. Chem. Soc., Faraday Trans.* **1991**, 87, 1905. (f) Kapoor, S. *Langmuir* **1998**, *14*, 1021.

(11) Hada, H.; Yonezawa, Y.; Yoshida, A.; Kurakake, A. *J. Phys. Chem.* **1976**, *80*, 2728.

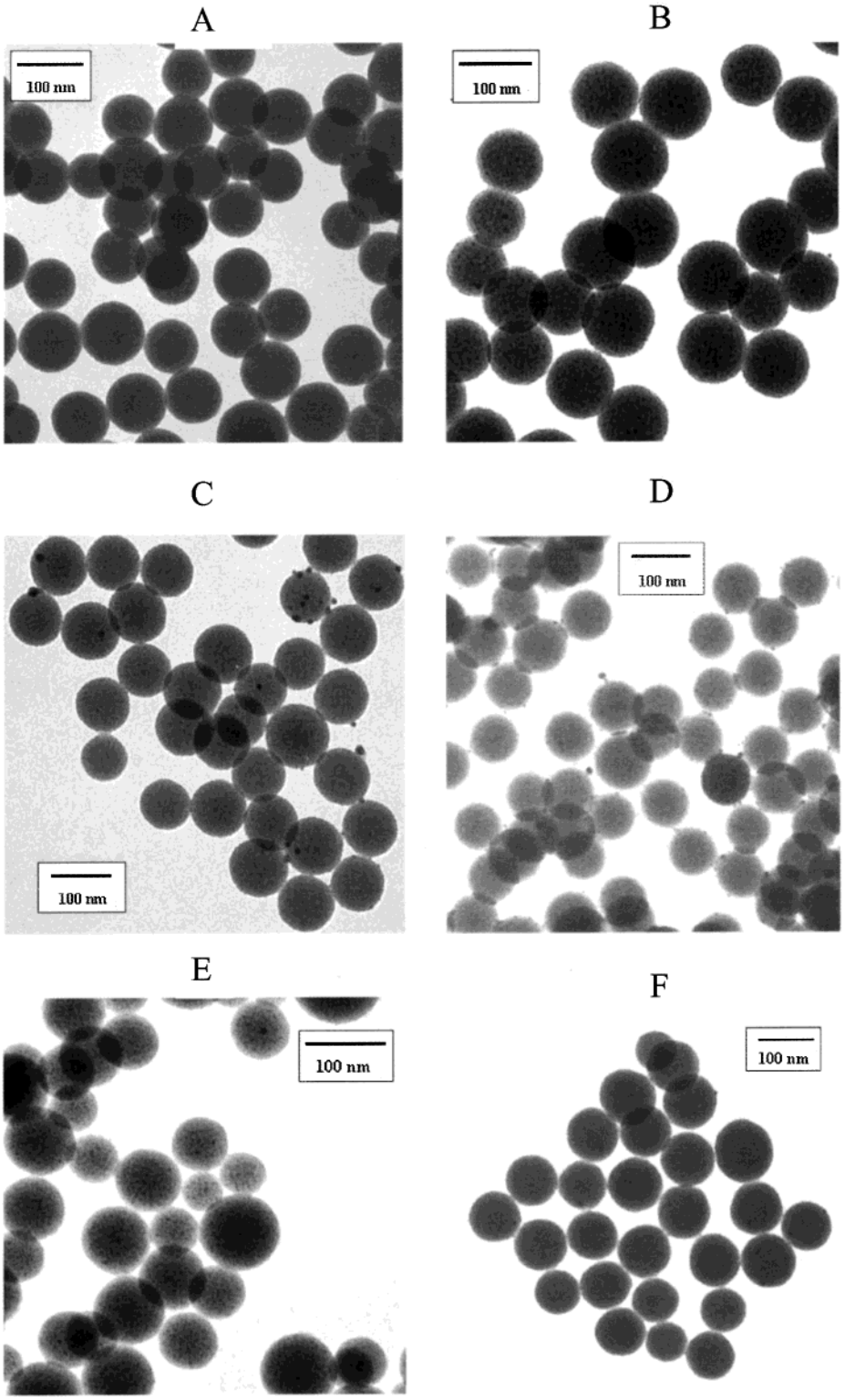

Figure 1. (A) TEM picture of reaction product not illuminated with UV light. A freshly prepared Ag^+ solution was used. There are no Ag inclusions visible in the SiO_2 spheres. $d_{sphere} = 85 \pm 9.5$ nm. (B) TEM photograph of colloidal particles formed during a 24 h reaction illuminated for the first 12 h with UV light. A freshly prepared Ag^+ solution was used. The monodisperse SiO_2 spheres show homogeneous incorporation of Ag quantum dot inclusions. $d_{sphere} = 95 \pm 9.3$ nm, $d_{Ag} = 2-5$ nm. (C) TEM of the reaction product of a 24 h reaction where UV illumination occurred only during the last 12 h. A freshly prepared Ag^+ solution was used. Ag quantum dots are incorporated in the SiO_2 spheres and on the sphere surfaces. $d_{sphere} = 87 \pm 6.5$ nm, $d_{Ag,\ inner} = 2-4$ nm, $d_{Ag,surface} = 5-10$ nm. (D) TEM of the reaction product of a 24 h reaction where the UV illumination only occurred during the last 4 h. A freshly prepared Ag^+ solution was used. Ag quantum dots are mainly incorporated around the sphere surfaces. $d_{sphere} = 91 \pm 6.9$ nm, $d_{Ag,surface} = 3-10$ nm. (E) TEM of the reaction product of a 24 h reaction where UV illumination occurred only during the first 4 h. The Ag quantum dots are concentrated in a region close to the SiO_2 sphere center. Few quantum dots occur in the outer SiO_2 sphere shell. $d_{sphere} = 74 \pm 13$ nm, $d_{Ag} = 2-5$ nm. (F) TEM of the reaction product of a 24 h reaction using an aged $AgNO_3$ solution in the absence of light illumination. A few Ag quantum dots incorporate into the SiO_2 spheres. $d_{sphere} = 81 \pm 7.8$ nm, $d_{Ag} = 2-5$ nm.

We can prepare fresh silver nitrate solutions that can be photoreduced by visible light. For example, if we initially illuminate a freshly prepared silver nitrate solution with UV light for 15 min and then use this solution in our microemulsion

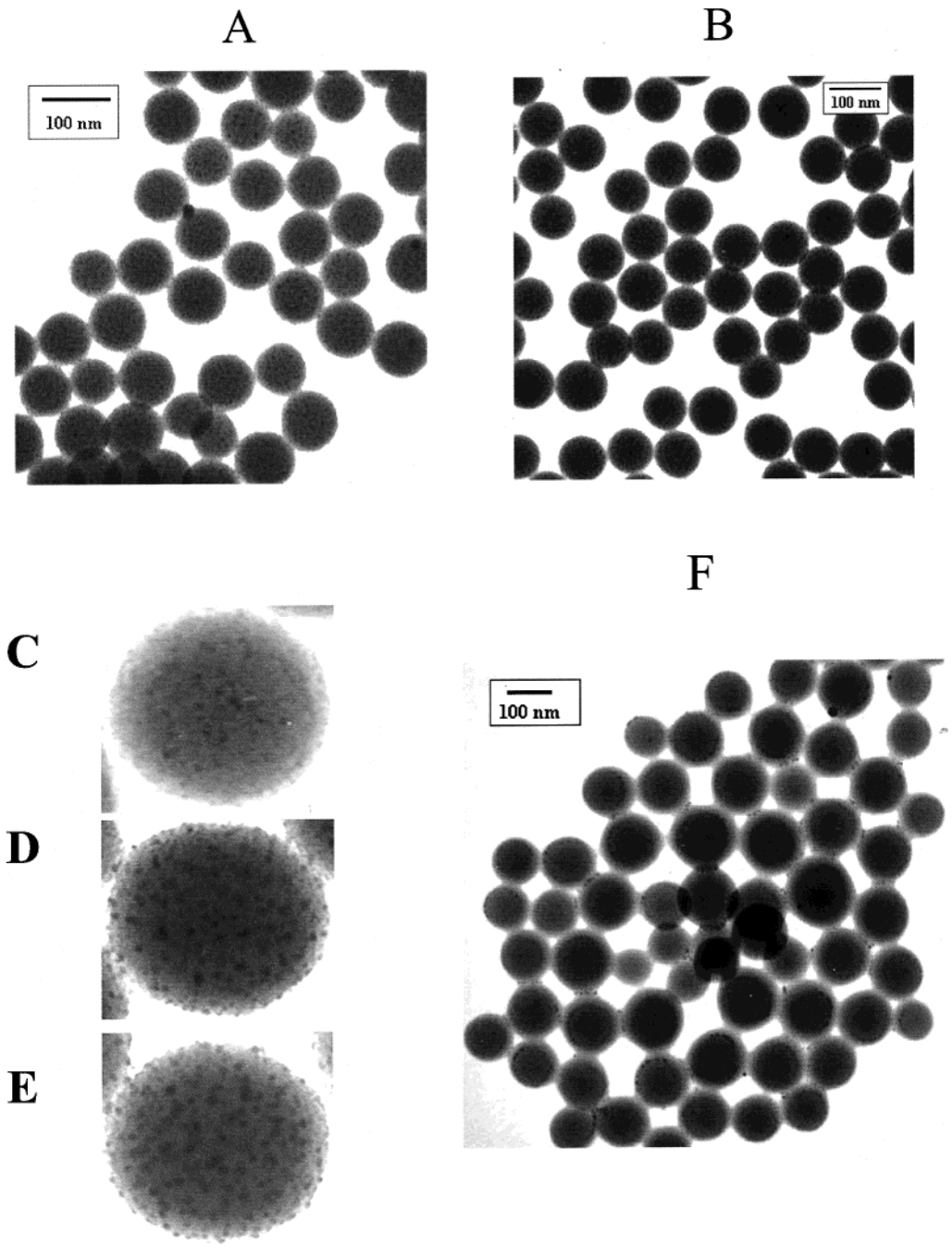

Figure 2. (A) TEM of reaction product of a 24 h reaction using an aged $AgNO_3$ solution illuminated for the first 12 h with visible light. The monodisperse SiO_2 spheres show a homogeneous incorporation of Ag quantum dot inclusions. $d_{sphere} = 78 \pm 5.4$ nm, $d_{Ag} = 3-8$ nm. (B) TEM of reaction product of a 24 h reaction where a freshly prepared $AgNO_3$ reaction solution was first illuminated for 15 min with UV light and then the microemulsion reaction mixture was illuminated for the first 12 h with visible light. The monodisperse SiO_2 spheres show a homogeneous incorporation of Ag quantum dot inclusions. $d_{sphere} = 82 \pm 5.8$ nm, $d_{Ag} = 3-8$ nm. We measured the Ag quantum dot loading by absorption spectroscopy and titration. Our absorption measurements, which utilized the absorption of similarly sized pure silver quantum dots in water, as a reference indicate a loading of ~1.5 wt %. For the titrations nitric acid was used to extract the silver from the composite colloidal particles, then ferric ammonium sulfate was added as an indicator and the silver ion was titrated with potassium thiocyanate. We measured a loading of ~1%. Magnified TEM images of Ag@SiO_2 composite particles: (C) 2−5 nm Ag quantum dots were formed by reduction with UV light (Figure 1B). (D) 3−8 nm Ag quantum dots were formed by reduction of an aged Ag^+ reaction mixture with visible light (Figure 2A). (E) 3−8 nm Ag quantum dots are formed by the visible light reduction of a fresh Ag^+ reaction mixture, where the Ag^+ solution was initially illuminated for 15 min with UV light (Figure 2B). (F) TEM of the reaction product of a two-step reaction. Pure SiO_2 spheres were first produced in the absence of Ag^+. After 20 h $AgNO_3$ and more TEOS were added, and the reaction was continued under UV illumination for another 24 h. The Ag quantum dots mainly incorporate in the outer shell of the SiO_2 spheres. $d_{sphere} = 92 \pm 11$ nm, $d_{Ag} = 2-5$ nm.

during the formation of silica spheres, we observe facile visible light silver photoreduction. This creates silica spheres which contain homogeneous inclusions of Ag quantum dots (Figure 2B). The visible light-reduced Ag quantum dots are larger (3−8 nm, Figure 2, B and A) than those reduced by UV light (2−5 nm, Figure 1B), as is most clearly observed in Figure 2C−E. Larger quantities of Ag quantum dots (up to 2−3 wt %), can be incorporated in the SiO_2 spheres by using visible wavelength

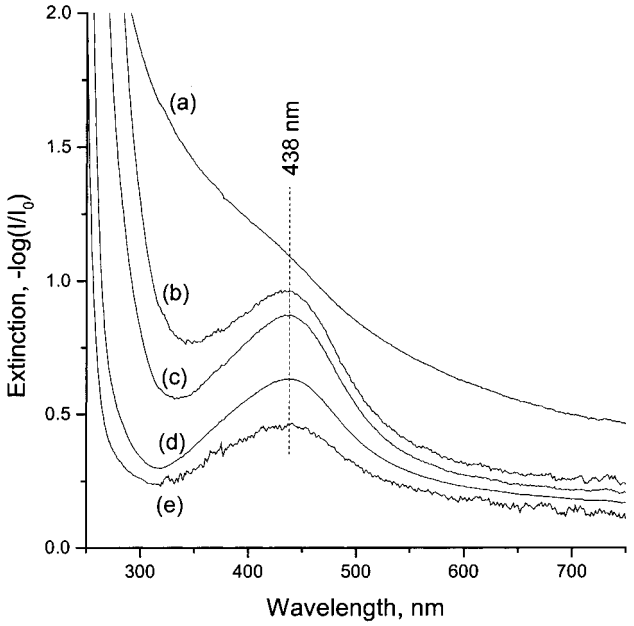

Figure 3. UV−visible extinction spectra of the Ag@SiO_2 composite colloid (95 ± 9.3 nm diameter SiO_2 sphere with homogeneous Ag quantum dot inclusions shown in Figure 1B). (a) in water $n = 1.337$, and in DMSO−water mixtures, (b) $n = 1.459$, (c) $n = 1.467$, (d) $n = 1.472$, (e) $n = 1.478$.

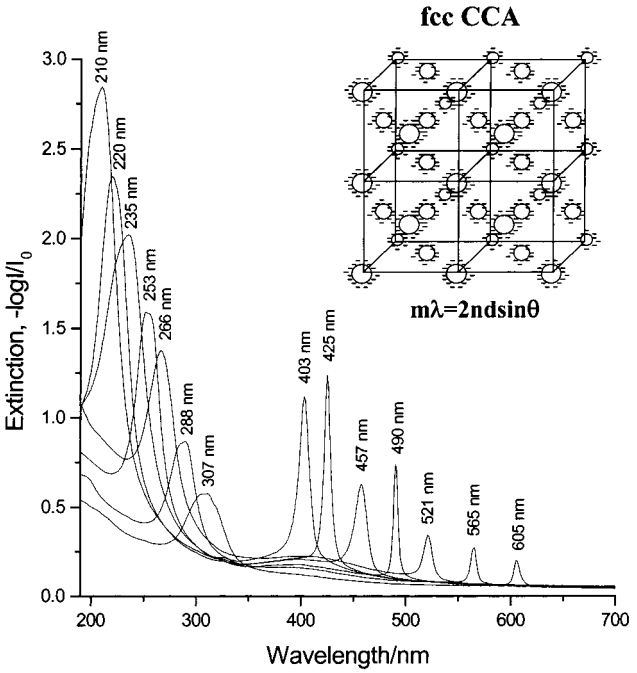

Figure 4. UV−visible extinction spectra of CCA of Ag@SiO_2 composite colloid (95 nm diameter SiO_2 spheres with ~1.5 wt % homogeneous Ag quantum dot inclusions) at different particle concentrations (vol %): 7.45, 6.61, 5.50, 4.43, 3.38, 2.34, and 2.12. The CCA thickness is 125 μm.

reduction. Thus, it appears that the aged silver nitrate solutions contain silver clusters which can absorb visible light and permit the further reduction of silver ions.

We also utilized a two-step synthesis to produce Ag@SiO_2 spheres where the Ag quantum dots occur in the outermost SiO_2 shell (Figure 2F). The reaction was initiated by using 12.0 mL of TEOS in the absence of Ag^+ ions. After 20 h, 0.85 g of $AgNO_3$ was dissolved in the microemulsion and then 8.0 mL of TEOS was added dropwise over 30 min under UV light illumination. The reaction continued for another 24 h.

Figure 3 shows the UV−visible extinction spectra of the Ag@SiO_2 colloid shown in Figure 1B. The strong light scattering from these ~95 nm spheres in water makes it difficult to observe the Ag quantum dot surface plasmon resonance absorption (curve a in Figure 3). However, this plasmon resonance is easily observed if we match the refractive indices of the colloidal particles by using a DMSO−water mixture (curves b−e in Figure 3). The Ag plasmon resonance exhibits a maximum at 438 nm.

We expect to see little change in the Ag quantum dot plasmon resonance frequency as the solvent refractive index changes between 1.45 and 1.48, given that, at most, there exists only a 20% silica pore volume. Theory indicates less than a 0.5 nm shift should occur for this small refractive index change.[12]

Most of our synthesized Ag@SiO_2 colloids show polydispersities in the range of 10−20% as measured by dynamic lighting scattering. The light scattering polydispersity values are usually lower than the TEM polydispersity values ($\sigma/\langle d\rangle$). The sphere sizes measured by light scattering are usually 20−60% larger than those from TEM measurements.

The particle polydispersity can be improved by particle size fractionation. For example, the Figure 1B colloid had an original diameter of 142.9 nm (from light scattering measurement) and a 19.7% particle polydispersity. We removed the larger particles by centrifuging the cleaned colloidal aqueous suspension at 1200*g* for 10 min and discarding the sediment. We then removed the smallest particles by centrifuging the suspension at 13000*g* for 10 min and discarding the supernatant. The remaining particles show a particle diameter of 147 nm and a polydispersity of 9.8%.

We further cleaned these colloidal particles by redispersing them in water and dialyzing them with 50 000 molecular weight cutoff dialysis tubing until the conductivity of the colloid was below 1 μS. This removed excess ions and surfactants. The dialyzed suspension was then placed in contact with mixed-bed ion-exchange resin.

After being shaken with the ion-exchange resin, the Ag@SiO_2 composite colloid suspension became iridescent, indicating that the particle suspension self-assembled into a crystalline colloidal array (CCA). The fact that these cleaned monodisperse colloidal particles readily from CCAs indicates that the colloidal particles have high surface charge.

Zeta potential measurements show ζ potentials of −56.46 ± 1.06 mV, which is significantly higher than the value of −40.67 ± 0.37 mV for pure SiO_2 spheres. This indicates that incorporation of the Ag quantum dots increases the negative charge of the SiO_2 spheres. Matijević et al. earlier reported that inclusion of single Ag core increased the electrophoretic mobility of the Ag@SiO_2 composite particles, compared to plain SiO_2 particles.[6] Pure SiO_2 colloids have negatively charged surfaces because of surface $Si-O^-$ groups. The additional negative charge of the Ag@SiO_2 composite particles presumably results from the negative charges of the Ag quantum dot inclusions.[6,13,14]

(12) (a) Kreibig, U.; Vollmer, M. *Optical Properties of Metal Clusters*; Springer Series in Materials Science, Vol. 25; Springer: New York, 1995. (b) Mulvaney, P. *Langmuir* **1996**, *12*, 788. (c) Kreibig, U.; Fragstein, C. V. *Z. Phys.* **1969**, *224*, 307. (d) Charlé, K. P.; Schulze, W. *Ber. Bunsen-Ges. Phys. Chem.* **1984**, *88*, 350. (e) Kawabata, A.; Kubo, R. *J. Phys. Soc. Jpn.* **1966**, *21*, 1765.

(13) Wang, W.; Efrima, S.; Regev, O. *Langmuir* **1998**, *14*, 602.

(14) Ung, T.; Giersig, M.; Dunstan, D.; Mulvaney, P. *Langmuir* **1997**, *13*, 1773.

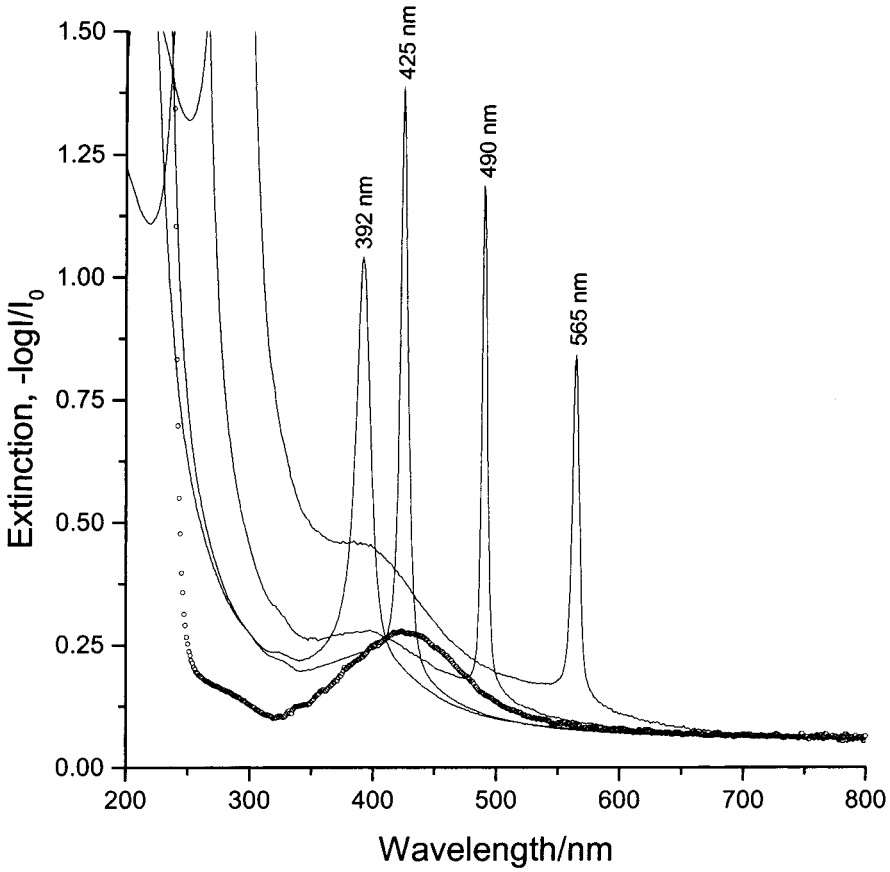

Figure 5. Comparison of extinction spectra of CCA of 95 nm diameter Ag@SiO$_2$ composite colloids at different particle concentrations (solid lines) to the extinction spectrum of a random dispersion of the particles in a $n = 1.47$ water−DMSO refractive index matching solvent (heavy line). The extinction spectra are normalized to the particle concentration of the random refractive index matched dispersion (7.43 vol %).

The CCA was injected into a cell consisting of two quartz plates, separated by a 125 μm Parafilm spacer for the UV−visible spectroscopic measurement. The CCA normally self-assembles with its highest particle density planes (the *fcc* (111) or *bcc* (110) planes) parallel to the quartz cell surface.[15]

Figure 4 shows the extinction spectra of CCA of these particles at different particle concentrations. The CCA Bragg diffract light, giving rise to intense peaks between 380 and 620 nm. The sharp diffraction peaks arise from the *fcc* 111 planes, while the peaks below 350 nm, at about half the wavelength of the *fcc* 111 plane first order visible diffraction bands, derive from diffraction from a set of higher-order lattice planes which are fortuitously oriented to fulfill the Bragg condition.[16] The diffraction bands shift to shorter wavelength as the concentration increases due to the decreased lattice spacing as the particle concentration increases.[15]

Figure 5 compares the extinction spectra of CCAs at different particle concentrations to the extinction spectrum of a random dispersion of identical particles (7.43 vol %) in the refractive index matching solvent (Figure 3). The diffraction extinction spectra were normalized to the 7.43 vol % particle concentration of the random dispersion of refractive index matched particles.

There is some attenuation of transmission for wavelengths shorter than the 111 plane diffraction, presumably due to disorder in the *fcc* crystal. The degree of disorder is very sample-dependent, which gives rise to a variable extinction on the short wavelength side of the 111 plane diffraction.

An important feature shown in Figure 5 is that the extinction of the plasmon resonance in the random dispersion at wavelengths longer than ~440 nm is greater than that observed for the *fcc* crystals with diffraction peaks at 490, 425, and 392 nm. This indicates a decreased plasmon absorption in these ordered diffracting samples.

Figure 6 shows the dependence of the extinction spectrum of a series of CCA, which are identical, except that they were prepared with different degrees of disorder, as evident from their variable 408 nm peak diffraction extinction and bandwidth and the disorder-induced shorter wavelength extinction. The larger the extinction of the 408 nm diffraction peak, the better the crystal ordering and the smaller the longer wavelength plasmon resonance absorption.

Figure 6 also shows that the Ag quantum dot plasmon resonance extinction around 450 nm is significantly below that of the random dispersion of particles for the well-ordered diffracting CCA, while they approach being identical for the poorly ordered samples. This indicates that the *fcc* crystal array ordering impacts the plasmon resonance absorption.

Figure 7 shows that the angular dependence of the diffraction wavelength of a single well-ordered CCA sample follows Bragg's law, where the diffracted wavelength decreases as the crystal is tilted from the normal:[15b]

$$m\lambda = 2nd \sin \theta$$

(15) (a) Clark, N. A.; Hurd, A. J.; Ackerson, B. J. *Nature* **1979**, *281*, 57. (b) Carlson, R. J.; Asher, S. A. *Appl. Spectrosc.* **1984**, *38*, 297. (c) Rundquist, P. A.; Photinos, P.; Jagannathan, S.; Asher, S. A. *J. Chem. Phys.* **1989**, *91*, 4932. (d) Kesavamoorthy, R.; Tandon, S.; Xu, S.; Jagannathan, S.; Asher, S. A. *J. Colloid Interface Sci.* **1992**, *153*, 188. (e) Asher, S. A.; Holtz, J.; Weissman, J.; Pan, G. *MRS Bull.* **1998**, 44.

(16) Liu, L.; Li, P.; Asher, S. A. *J. Am. Chem. Soc.* **1997**, *119*, 2729.

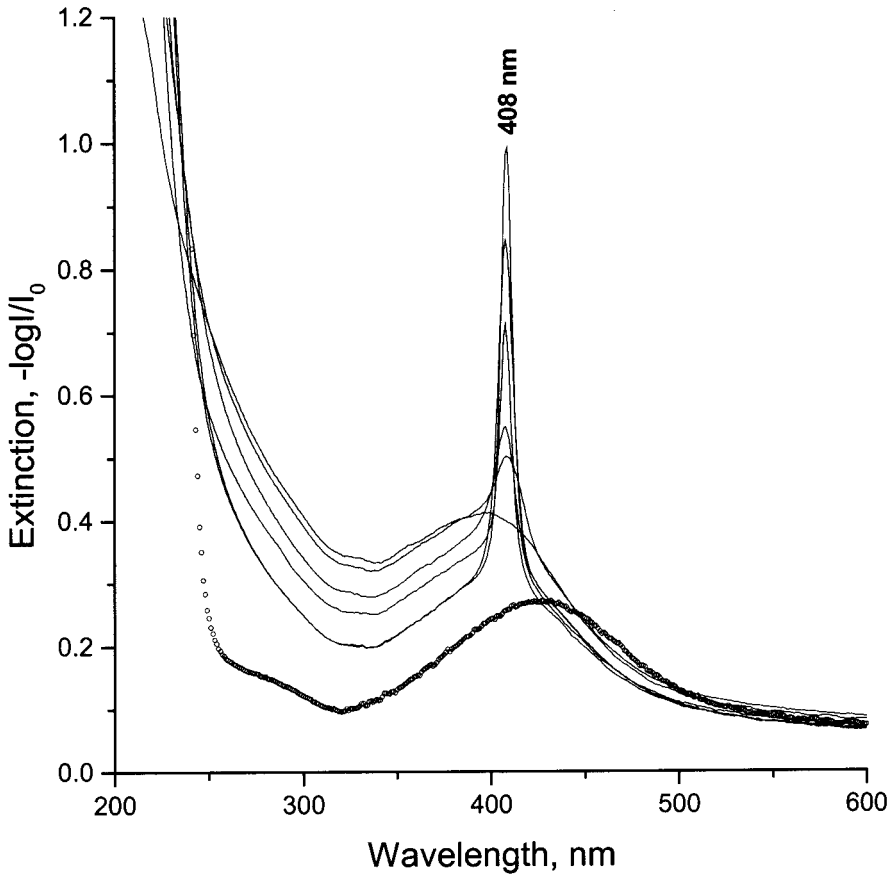

Figure 6. Comparison of extinction spectra of CCA of 7.22 vol % of 95 nm diameter Ag@SiO_2 composite colloids with different amounts of disorder (solid lines) to the extinction spectrum of a random dispersion of these colloids (7.22 vol %) in a $n = 1.47$ water−DMSO refractive index matching solvent (heavy line). The CCA thickness is 125 μm.

where m is the order of diffraction, λ is the diffracted wavelength in vacuum, n is the refractive index of the system, d is the spacing between diffracting planes, and θ is the Bragg glancing angle between the incident light propagation direction and the diffracting planes. Because the beam is traversing the sample off of the normal by a maximum of ∼26°, we expect a maximum ∼10% increase in the plasmon absorption at the maximum tilt angle.

The plasmon resonance absorption in these samples is evident as a broad shoulder at ∼430 nm. At wavelengths longer than ∼450 nm all CCA spectra show less extinction than does the random dispersion plasmon resonance absorption. Below 430 nm the extinction spectra show a pattern that could be interpreted as an increased plasmon resonance extinction. Unfortunately, this issue is not completely unambiguous; this increased extinction could also derive from a fortuitous angular dependence of the sample disorder scattering.

Thus, Figures 5−7 indicate that the Ag plasmon resonance extinction depends on the Bragg diffraction condition. Light transmission at a wavelength on the red side of the plasmon resonance maximum experiences an extinction less than that of a pure random dispersion of the Ag@SiO_2 particles. In contrast, Figure 7 may suggest that light on the blue side of the plasmon resonance maximum experiences an increased extinction.

This phenomenon is somewhat reminiscent of the Borrmann effect[17] occasionally observed in X-ray diffraction. In this case the diffraction condition sets up a standing wave involving the diffracted and incident light. For scattering from atoms by X-rays the electric field maximum can occur either in the planes where the atoms lie, where the absorption would be a maximum, or it can occur between the planes where the absorption would be a minimum (Figure 8).

Diffraction band gap theory suggests that the long wavelength side of the band edge should localize the electric field in the higher dielectric constant region of the diffracting array.[18] The real part of the dielectric constant of the silver quantum dots is expected to be large and negative close to the plasma resonance frequency. Simple Mie theory[12a] indicates that close to the plasmon frequency, the dielectric constant for an isolated metal particle, $\epsilon = -2\epsilon_m$, where ϵ_m is the dielectric constant of the medium in which the quantum dot is imbedded (silica). In fact, our situation is more complex since these quantum dots can occur in the form of aggregates.

The negative contribution of the dielectric constant of the silver quantum dots will decrease the average Ag@SiO_2 particle dielectric constant, which will significantly decrease the average Ag@SiO_2 particle refractive index. Thus, the effective refractive index of the Ag@SiO_2 particles may become significantly smaller than that of the water medium.

Thus, the standing wave electric field could have its maxima in the mainly aqueous region away from the silver quantum dots. Thus, from this consideration, we expect to observe a decrease in plasmon absorption on the red edge of the band gap. However, our actual case is much more complex than the simple cases previously treated. The plasmon resonance is inhomogeneously broadened by the distribution of silver nano-

(17) Batterman, B. W.; Cole, H. *Rev. Mod. Phys.* **1964**, *36*, 681.

(18) Joannopoulos, J. D.; Meade, R. D.; Winn, J. N. *Photonic Crystals;* Princeton University Press: Princeton, 1995.

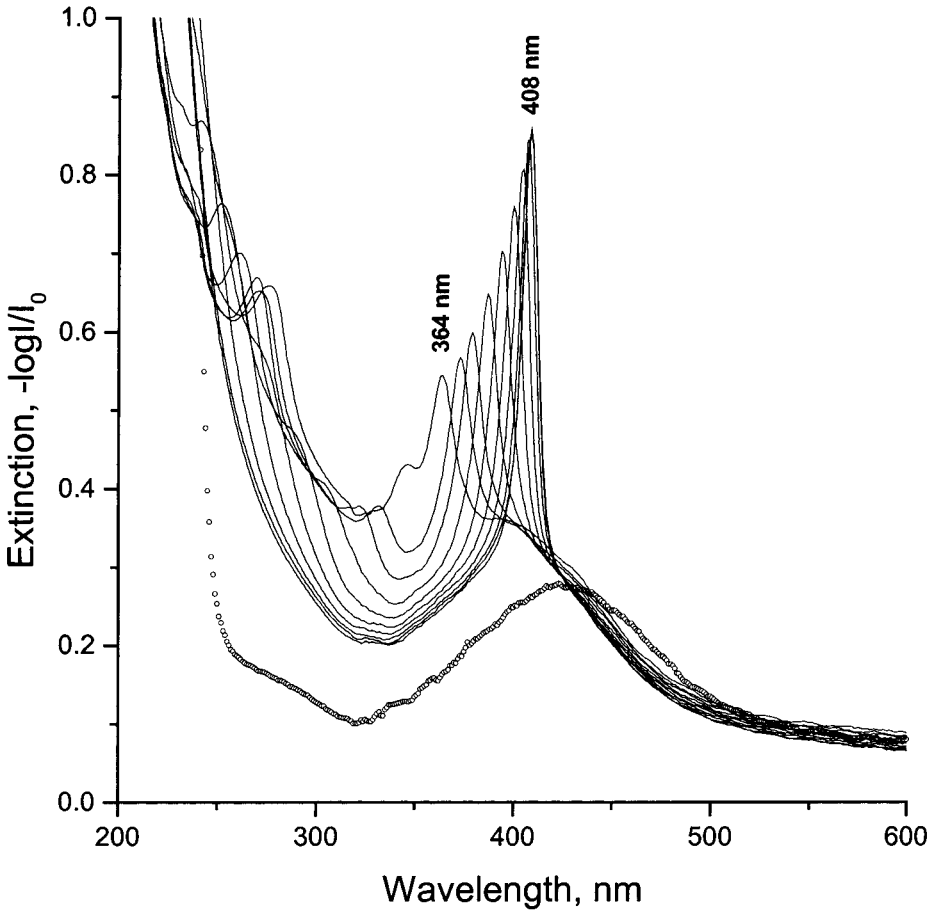

Figure 7. Extinction spectra of a 7.22 vol % CCA of 95 nm diameter Ag@SiO$_2$ composite colloids obtained at different light external incident angles to the 111 plane (solid lines, 90°, 85°, 80°, 75°, 70°, 65°, 60°, 55°, and 50°). Also shown is the extinction spectrum of a random dispersion of these same particles (7.22 vol %) in a $n = 1.47$ water−DMSO refractive index matching solvent (heavy line). The CCA thickness is 125 μm.

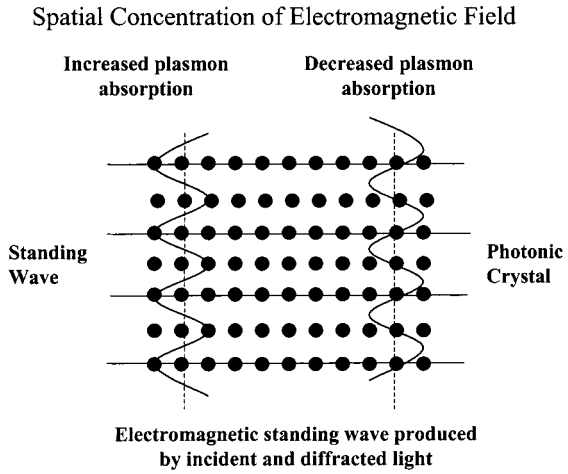

Figure 8. Schematic illustration of the Borrmann effect in a CCA photonic crystal. A standing wave is produced by the coupled incident and diffracted light. If the electric field maximum lies in the particle planes the absorption is a maximum, while if the electric field maximum lies between the particle planes, the absorption is a minimum.

particles, and the silver particle dielectric constant may be influenced by the collective excitation of the aggregate of silver nanoparticles. The diffraction is inhomogeneously broadened by crystal mosiacity and the Debye−Waller effect which results from the distribution of positions of the particles around their lattice sites. Further, the diffraction occurs somewhere between the thick crystal and thin crystal limit[15c,19] since the extinction has a value of ~1.

This Borrmann-like phenomenon may have important implications for nonlinear optical materials, since the ability of photonic materials to concentrate the electric field in particular regions of space could be used to dramatically increase their apparent material optical nonlinearities.

We believe that this is the first demonstration of the Borrmann-like effect, where the incident electric field becomes localized in a standing wave in a photonic crystal. Further work is necessary to understand the observed phenomena.

Acknowledgment. We acknowledge helpful conversation with Richard Van Duyne, George Chumanov and Joseph Haus. We also acknowledge support for this work from NSF Grant (CHE-9813295), ONR Grant (N00014-94-1-0592), and ARO Grant (DAAD16-99-R-1006).

JA011262J

(19) Zachariasen, W. H. In *Theory of X-ray Diffraction in Crystals*; Dover Publications: New York, 1945.